Dynamic Functional Connectivity Graph for Assessing Cascading Events in Power System

Tabia Ahmad
Panagiotis N Papadopoulos
Department of Electronics and Electrical Engineering
University of Strathclyde
Glasgow, United Kingdom
{tabia.ahmad, panagiotis.papadopoulos}@strath.ac.uk

***Abstract*—During power system cascading disturbances it becomes crucial to quickly identify the vulnerable transmission interconnections. Understanding the impact of a triggering outage on these critical interconnections is important for enhancing situational awareness and taking targeted control actions. This paper proposes a new machine learning (ML) based graph-theoretic approach for learning the dynamic functional connectivity (DFC) between power system buses with respect to their vulnerability to cascading failures (CF). The learnt DFC graph is then used to characterise vulnerable regions of the power-system using complex network theory based indices. A key feature of the proposed DFC graph is that it takes into account detailed power system dynamics and the action of protection devices when deriving the DFC, going beyond a static representation of the power system graph based on electrical admittances. Multiple operational scenarios for load and renewable generation are also considered when doing so. The proposed algorithm is validated for a dynamic model of the IEEE-10 machine 39 bus system with Type IV wind generation.**

***Index Terms*—Cascading events, complex network theory, power system dynamics, spatio-temporal graph, deep learning.**

I. Introduction

Interconnected power systems operating closer to their limits as well as large-scale integration of renewable energy resources have introduced significant complexities and uncertainties in the power systems; requiring the future power system to be not only resilient to failures but also capable of being steered to a desired state through targeted power system control. Of particular concern for power system operators is the possibility of cascading failures (CF) – a quick succession of multiple component failures usually triggered by one or more disturbance events such as extreme weather, equipment failure, or operational errors [1]. This may also lead to a blackout causing huge economic and social costs. The outage process in cascading failures can be divided into two phases: the *slow* cascade and *fast* cascade phases [2], [3]. The latter phase, often driven by the transient dynamics of the system, may result in power system collapse or major load shedding. However, it is possible for the system operators to take preventive remedial actions to arrest their propagation and possible manifestation into blackouts. Detection of vulnerable power system components and their spatial location is thus critical for resiliency of modern power systems.

A. Literature Review

Investigating the vulnerability of renewable-integrated power systems to CF using a high fidelity dynamic model incurs huge computational burden which often increases exponentially with the number of components [4]. Cascading events in power systems exhibit non-local propagation patterns which makes the purely structural analysis of failures unrealistic [5]. Moreover, it is evident from post-mortem analysis of several blackouts triggered by cascading failures, that the effect of complex (rotor angle, voltage and frequency) dynamics, their typical dynamic controllers and discrete protection devices need to be taken into account for accurate representation of CFs [6]. There are various techniques present in literature, which model and analyse the underlying interactions among power system components with respect to CF. While the knowledge of these interactions are important to characterise vulnerable spatial locations, this may not be readily available from mere knowledge of power system physical models and topology. Such techniques can be broadly classified as those based on power system time-domain simulation [7], deterministic analytical models [8], [9], probabilistic models [10], and graph-based models [11]–[13]. Among these categories, graph-based methods have attracted a lot of attention due to their natural applicability to a power system network. Many graph-based models were developed with vulnerability indices based on the physical topology of the power system (whereby the connections among the graph nodes represent the actual physical connections among the components of the power system) [14]. Nonetheless the studies in [5], [15] showed the lack of strong connection between the physical topology of the system and cascading failure propagation in power systems. These influences and component interactions during the cascade process may occur both locally and at distance due to the physics of power flow as well as other functional dependencies among power system components [9]. Studies to reveal these complex and hidden interactions are focused on extracting

This work was supported by UKRI Future Leaders Fellowship MR/S034420/1 (P. N. Papadopoulos, T. Ahmad). All results can be fully reproduced using the methods and data described in this paper and references provided.

the underlying graph of interactions among the components of the system [13]. Extended topological indices [16]–[19], i.e., integrating specific physical behaviours of power system into the complex network theory based approaches, based on admittance, current, and line-flow graphs have been proposed. For example, [20] introduces the capacity of transmission lines and generators to improve the maximum flow approach. In summary most of the works proposed in literature make use of the structural power-system graph while few others proposed metrics calculated using a power-flow based graph but their edges are weighted by the average value of power-flow. These weighted graphs include no temporal information, which might be crucial in analysing CF. Albeit, there are few works present in literature that make use of graph-theoretic approaches based on dynamic connectivity of power system generators or loads, they make use of a reduced power system graph for studying different pathways to failure [21], [22]. In addition to this, another challenge is to include the effect of operating states of the power system (i.e., renewable generator output and load levels) which may change before the cascading outage occurs. In different operating states, the vulnerable locations of power systems may be different and it may be very time-consuming and impractical to assess all possible initial boundary conditions in operational planning/real-time applications, hence the premise of machine learning (ML) for such inference tasks is of interest.

B. Key Contributions

In this work we utilise spatio-temporal graph convolutional networks (st-GCN) for predicting whether an operational scenario and initial failure will lead to CF or not, while also learning an improved connectivity matrix leveraging post-fault dynamic power system features and network topology in the form of bus admittances. Building on our previous work [23], the graph induced by this learnt connectivity matrix is sparsified and this graph is referred to as the dynamic functional connectivity (DFC) graph. The DFC graph is further used to calculate complex network theory based indices and systematically compared against the indices obtained for a static admittance based graph. Inferences are then drawn on how the DFC graph can provide complementary and additional insights to better characterise vulnerable regions of the power system with respect to CFs. The proposed algorithm is validated for a dynamic model of the IEEE-10 machine 39 bus system with Type IV wind generation and protection devices.

Remainder of the paper is structured as follows: Section II briefly introduces graph-theoretic modelling of power system and the proposed methodology of learning DFC graph. Section III showcases the numerical case studies while Section IV discusses the results. Finally Section V includes conclusion and future work.

II. Methodology

This work proposes learning a functional connectivity graph pertaining to dynamic CF using spatio-temporal power system features under different operational scenarios and initial contingency. First, power system spatio-temporal graphs are introduced and then spatio-temporal graph convolution (st-GC) operation is defined on them. Next, the training of st-GCN based learning framework with an edge-importance matrix is enumerated. The learning framework uses st-GC in each layer and models the importance of graph edges in the decision process across layers. Finally, the process of creating DFC graph from edge-importance matrix is discussed in this section.

A. Spatio-temporal Power System Graphs

Conventionally, the power system is modelled as a weighted, undirected graph, $\mathcal{G}$, whereby nodes, $\mathcal{N}$ are represented by power system buses. The edges of graph, $\mathcal{E}$ are represented by transmission lines and transformers. Let $\mathcal{N} \in (n_g, n_l)$ be the number of buses equipped with generator and load respectively. The spatial connectivity between different nodes of the graph is represented by the weighted adjacency matrix, A. In this work, it is assumed that each bus is equipped with a phasor measurement unit (PMU) and time-varying voltage magnitudes, $V^{mag}(t)$ at each bus are captured. The presence of features at all N buses (no missing values) ensures a good learning outcome for a $N \times N$ sized system, but practically speaking, the current framework can also utilise a reduced dimension power system graph, for example with features present at only generator buses. Specifically, $V^{mag}(t) = \left\{v_{t,i}^{mag} | t = 1, 2, ..., T; i = 1, ...N\right\}$ represent a set of voltage magnitudes assumed to be collected from N PMUs and for T time points. The spatio-temporal graph is constructed in two steps. First, nodes of the spatial graph at one time instant are connected with edges according to A as in a conventional power system graph. Then each node in the spatial graph is connected to the same node for the consecutive time instant. For the spatio-temporal graph thus formed, the edge-set is composed of two subsets: the first subset depicts the intra-power system connection at each time instant, denoted as $E_S = \{v_{ti}v_{tj} | (i, j) \in \mathcal{N}\}$ and the second subset contains the inter-time edges, which connect the same nodes at consecutive time instants as $E_T = \left\{v_{ti}v_{(t+1)i}\right\}$. Therefore all edges in E_T for one particular node i represents its trajectory over time. The goal of st-GCN based graph learning algorithm is to utilise the spatio-temporal graph to compute latent relationship between power-system buses for the CF problem. In this paper, this relationship is termed as *power system DFC* and the graph induced by it is referred to as the DFC graph. This has been illustrated in Fig. 1 which represents a high-level framework of the proposed scheme.

B. Network Architecture for Spatio-Temporal Graph Convolution Learning

To define convolution on spatio-temporal graphs, the concept of spatial and temporal neighbourhoods which refers to data of neighbouring nodes and at neighbouring time instants, introduced by [24] is utilised. The spatio-temporal neighbourhood of node v_{ti}, denoted by $\Lambda(v_{ti})$ is defined as

$$\Lambda(v_{ti}) = \{v_{qj} | e(v_{tj}, v_{ti}) \leqslant S, |q - t| \leqslant |\mathrm{T}/2|\} \quad (1)$$

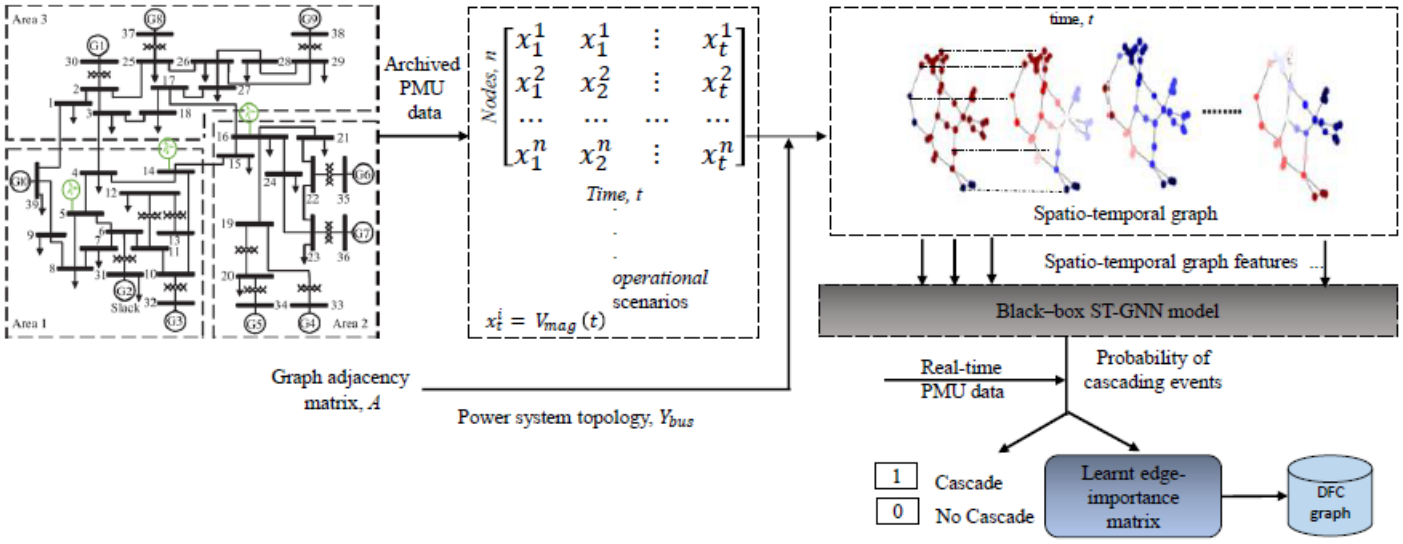

Fig. 1: Proposed st-GCN framework for learning dynamic functional connectivity whilst classification of scenarios which lead to cascading events

where S defines the size of the spatial neighbourhood (i.e., spatial kernel size), T the temporal neighbourhood(i.e., temporal kernel size) and $e(v_{tj}, v_{ti})$ denotes the minimum length of any path from v_{tj} to v_{ti}. Next, st-GC operation on node v_{ti} with respect to a convolutional kernel $w(.)$ and a normalisation factor $\mathcal{N}_{ti}$ which is equal to the cardinality of the corresponding sub-set, is given as

$$f_{out}(v_{ti}) = \frac{1}{\mathcal{N}_{ti}} \sum_{v_{qj} \in \Lambda(v_{ti})} f_{in}(v_{qj}) . w(v_{qj}) \qquad (2)$$

Adopting a similar implementation as in [25], the spatio-temporal convolutional kernel is approximated by decomposing it to a spatial graph convolutional kernel $W_{SG} \in R^{C \times P}$ represented in the spectral domain and a temporal convolutional kernel, $W_{TG} \in R^{M \times \mathrm{T}}$. It is clarified that $f_t \in R^{N \times C}$ denotes the C types of input features ($C = 1$ for the current work as only bus voltage magnitude features are used) of the N nodes at the t^{th} frame, $f'_t \in R^{N \times P}$ denotes the P output features. It is important to note that the current framework of spatio-temporal GCNs which benefits from the topology information, does not support complex features such as voltage phasor, hence either voltage magnitude or voltage phase angles can be used. The spatial graph convolution at time t is then defined with respect to the symmetrically normalised graph Laplacian matrix, $L = D^{-\frac{1}{2}} \tilde{A} D^{\frac{1}{2}}$, using the aforementioned weighted adjacency matrix with self-loops, $\tilde{A}$ (where $\tilde{A} = A + I$) as

$$f'_t = D^{-\frac{1}{2}} \tilde{A} D^{-\frac{1}{2}} f_t W_{SG} \qquad (3)$$

Next, the temporal convolution is performed on the resulting features. Standard 1D convolution $f'_t \odot W_{TG} \in R^{\mathrm{T} \times \mathrm{T}}$ is performed to derive the final output of st-GC for v_i. The output of the last st-GC layer is fed to a global average pooling and its output vector is transformed to class probabilities by a fully connected SoftMax layer with a sigmoid activation.

C. Edge-importance matrix

To determine the importance of spatial graph edges in defining class probabilities, a positive and symmetric "edge importance" matrix, $M \in R^{N \times N}$ is integrated into the model. This matrix is shared across all st-GC layers by replacing $\tilde{A}$ in (3) by $\tilde{A} \circ M$ where $\circ$ denotes the element-wise product. While performing spatial graph convolution on node i, the contribution from its neighbouring nodes, as defined by spatio-temporal neighbourhood, $\Lambda(v_{ti})$ will be re-scaled according to the importance weights learned in the i^{th} row of M. Finally the model is trained in an end-to-end manner by back-propagation using stochastic gradient descent (SGD).

D. DFC graph : graph sparsification via κ - neighbourhood

A salient feature of the proposed framework is that an edge-importance matrix is integrated into the model and learnt end-to-end as an additional trainable parameter within the st-GCN framework. Thus, the edge-importance matrix (or learnt adjacency matrix) takes into account information from both topology and dynamic behaviour of power systems. Incorporating this, not only leads to superior performance in terms of the downstream task of classifying scenarios leading to CF but this matrix can also be projected as a dynamic functional connectivity specific to cascading events [23]. It is a positively weighted, symmetric and dense (fully-connected) matrix. Using this matrix it is possible to produce a weighted graph representation of the most buses of the power network (and the dynamic components connected to them) with respect to their vulnerability to CF. The fully connected graph may be used to derive a sparse graph (similar to topological power system graph but re-weighted) using the κ - neighbourhood sparsification scheme [26]. To achieve this we keep the original nodes of the network and retain only the links with weights over a user-defined threshold κ in the learnt matrix M.

$$DFC = \begin{cases} m_{ij} & m_{ij} < \kappa \\ m_{ij} = 0 & m_{ij} \geq \kappa \end{cases} \quad (4)$$

where m_{ij} represents the weight of the edge connecting nodes i and j in the graph induced by M. The thresholdκ is chosen such that the number of edges remains the same as in the topological graph.

III. Case Studies

In order to predict the occurrence of *fast* CF in a comprehensive manner there is a need for detailed modelling of power system dynamics. It is also imperative to consider multi-time scale dynamics, the operation of protection devices, initial operating conditions governed by dispatch of generators and appropriate representation of system load and renewable generation for an accurate vulnerability assessment. In this work, root-mean square simulation (RMS) of a dynamic model for modified IEEE 39 bus 10 machine New England system with Type IV wind generation and protection devices is used to generate bus-voltage magnitude trajectories. The modified IEEE 39 bus 10 machine test case has been shown in Fig. 2. These time-domain trajectories known as *power-system features* are suitably pre-processed and resampled to a typical PMU reporting rate of 10 milli-sec [27]. These features are then used for the creating spatio-temporal graphs as described in Section IIA. Detailed modelling assumptions and choice of dynamic parameters for the test system are adapted from [28]. Three phase faults on transmission lines are simulated as initiating events, while considering load and RE variations to capture realistically, a number of operating conditions which lead to different dynamic response, when large perturbations such as line-trips are encountered. Faults on all 34 lines and step changes in load (ranging from 0.7 to 1.2 p.u. in steps of 0.1 p.u.) and wind energy generation (ranging from 0 to 1 p.u. in steps of 0.2 p.u.) leads to 44064 independent scenarios, out of which dynamic CF are reported in some cases, which are labelled as *unsafe*, while others are labelled as *safe*. In this work, a simple undersampling strategy is followed and a balanced dataset containing all unsafe cases and an equal number of safe cases, is created out of the total scenarios. It may be important to note that importance sampling techniques such as [29] may further be used to effectively sample important scenarios for CF, further enriching the learning set, which however is not the focus of the current work. The input weighted adjacency matrix, A for the st-GCN model is derived based on power-system bus admittance matrix, Y_{bus} as the graph Laplacian matrix. As a common assumption for high-voltage transmission networks, the resistance of the lines is ignored and only susceptances are considered in Y_{bus}. The input dataset is a three-dimensional tensor of order $[V \times N \times T_w] = [11000 \times 39 \times 10]$, where V is the vector of voltage magnitude recorded at $N = 39$ buses for 11000 cases and for $T_w = 10$ time-steps window. The size of the output vector is $[Y] = [11000 \times 1]$. In order to make the learning process robust and less prone to overfitting, stratified k-fold cross validation for $k = 5$ splits is used for different splits of training and testing data. With the prepared database and optimised filter parameters the st-GCN model is trained for learning the augmented connectivity (i.e. edge-importance matrix) as well as simultaneous binary classification of CF. Standard libraries in Pytorch [30] are used to implement the proposed st-GCN pipeline. To reduce uncertainty in the estimation caused by SGD, training is repeated over 20 independent runs and the *average* edge importance matrix over these independent runs is derived as the final outcome. In this work, all learning computations were performed on a Intel Xeon 3.90 GHz machine with 128 GB RAM, and an NVIDIA RTX A6000 GPU.

*1) **Model performance**:* After training the model, its performance on the test dataset is observed to confirm the credibility of the edge-importance matrix. Our findings show that the model achieves an accuracy of $97.10 \pm 1.03\%$ at the 95% confidence level, assuming independent trials. This is significantly improved from $92.89 \pm 7.11\%$, when the M-matrix was not being used at all.

*2) **Computational requirements**:* Major computational burden for the proposed framework involves that due to RMS time domain simulations of the modified test case and training of the st-GCN framework. Under the current simulation set-up in Digsilent Powerfactory, RMS time-domain simulation of each scenario with no CF takes an average of 22 seconds while a scenario with CF takes around 86 seconds. With increase in the number of buses (and effectively the number of dynamic components) the computational burden increases exponentially [4]. Nevertheless, with highly specialised high-performance computing architectures and parallelized simulation sub-routines this time has been shown to decrease [31], [32]. The computational complexity of st-GCN approximately scales as $O(T\mathcal{E})$, where T represents the length of time sequence and $\mathcal{E}$ denotes the number of edges of the spatial power system graph [33]. For the IEEE 10 machine 39 bus case study, the computational complexity in terms of floating point operations (FLOPs) is 4.86×10^9. The training time is 1.1 minutes and inference times (per example) is 0.17 ms. The training time of st-GCN model (although expected to be performed offline), is expected to increase linearly with system size, thereby suitable for practically large power systems. The inference times per example are also well within the PMU sampling time of 10 ms, thereby making the learning framework suitable for real-time inference too.

*3) **DFC graphs**:* The trained edge-importance matrix, is thus projected as DFC, in terms of vulnerability to CF. A sparse DFC graph (shown in Fig. 3(a)) is created from the fully-connected DFC graph after applying the sparsification technique discussed in Section II-D, using $\kappa = 0.57$. For comparison, a graph based on bus-admittance connectivity is also shown in Fig. 3(b). Here, the sky-blue solid circles representing the nodes of graph correspond to power system buses, denoted by $[B01, B02....B39]$, while the edges connecting the nodes correspond to lines, whose weights are given by the adjacent colourbar. It may not be appropriate to discuss the accuracy of learnt M-matrix because there is no ground truth

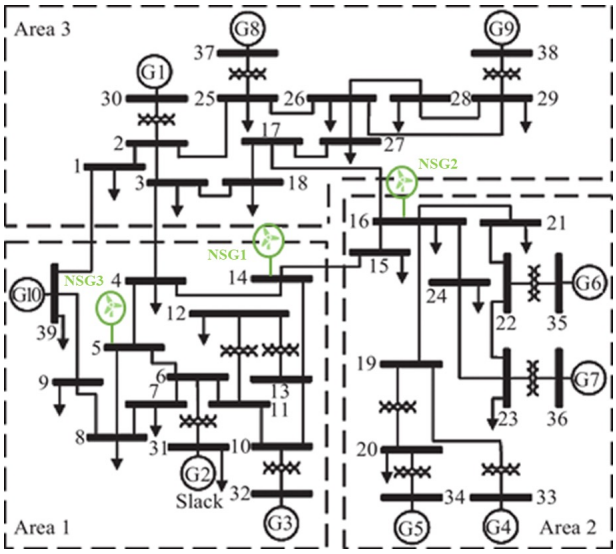

Fig. 2: Modified IEEE 10 machine 39 bus system with Type IV wind generation

about how the connectivity structure should be in order to maximise performance for the task of classifying cascading events. It is however, found to be correlated with the electrical connectivity (based on Y_{bus}) [23].

*4) **Complex network theory based centrality indices**:* In addition to superior performance on the downstream classification task, a key contribution of the proposed framework is that the learnt DFC graph is used to characterise vulnerable spatial locations of the power-system using complex network theory based centrality indices. These centrality indices are commonly used to understand and identify structural conditions that favours an edge or node to affect the behaviour of other elements. In this work node-centrality measures like degree, betweeness, closeness, and eigen-vector centrality [15] - briefly defined below, are calculated for the DFC graph and bus-admittance graph respectively. These node centrality indices are then used to infer the importance ranking of each node, with respect to their vulnerability to CF.

- Degree Centrality: For weighted power system networks, its degree centrality is related with how many links it connects and the connecting strength of each link. For a graph, $\mathcal{G} = (V, E)$, where V represents the set of nodes and E the set of edges, n is the total number of nodes, Laplacian $\mathcal{L}$, the degree centrality of a node v, $C_d(v)$ is defined as

$$C_d(v) = \frac{\|\mathcal{L}(v,j)\|}{n-1} \tag{5}$$

- Betweeness Centrality: This measure emphasises the distance of a vertex to all others in the network by focusing on the shortest distance from each vertex to all others. The betweeness of a node v, $C_b(v)$ is defined as the number of shortest paths between pairs of other vertices that run through v:

$$C_b(v) = \frac{\sum_{i \neq v \neq j \in V} \sigma_{ij}(v)/\sigma_{ij}}{(n-1)(n-2)/2} \tag{6}$$

where σ_{ij} depicts the number of shortest paths from i to j and $\sigma_{ij}(v)$ is the total number from the mentioned paths that pass through vertex v.

- Closeness Centrality: It is the average geodesic distance (i.e., shortest path length) between a vertex v and all the other vertices reachable from it:

$$C_c(v) = \frac{\sum_{j \in V \setminus v} d(v,j)}{n-1} \tag{7}$$

with d being the shortest path length between vertices v and j. However, this definition measures how "far away" a node is from the rest of the network instead of its closeness. Therefore a more appropriate quantity, $C_c^{'}(v)$ is defined by its reciprocal

$$C_c^{'}(v) = \frac{n-1}{\sum_{j \in V \setminus v} d(v,j)} \tag{8}$$

- Eigen-vector Centrality: It is a measure of the importance of a node in a network according to its adjacency matrix. Given a graph $\mathcal{G}$, its adjacency matrix A, its eigenvalue λ, and the corresponding eigenvector x satisfying $\lambda x = Ax$, then the centrality of a node v is defined as the v^{th} entry of the eigenvector x corresponding to the largest eigenvalue λ_{max}

$$C_e(v) = \frac{1}{\lambda_{\max}} \sum_{j=1}^{n} A(v,j) x_j \tag{9}$$

The rank Spearman correlation between the two sets of centrality measures is also calculated to observe if complementary and/or additional insights about vulnerability to CF can be drawn based on proposed DFC graphs.

IV. Results and Discussion

As noted in the Introduction, Y-bus based connectivity may not be a reliable metric for vulnerability assessment in the event of a CF involving *fast* failures due to tripping of protection devices and dynamic response of the power system. The vulnerability patterns derived using the proposed DFC graph on the other hand are consistent with the results of time-domain simulation using a full-dynamic model with the action of protection devices. A preliminary observation from the graphs based on DFC and Y-bus based connectivity as visualised in Fig. 3(a) and Fig. 3(b) respectively, is that there are more light-coloured links in the DFC graph which indicate higher edge-weights and hence higher number of strong connections than the Y-bus based graph. These indicate important connections in terms of propagation of CF. The dashed circles in Fig. 3(a) and Fig. 3(b) represent the buses/lines to which the components most frequently tripped are connected. For example, in the DFC graph shown in Fig. 3(a), links with higher edge-weights (i.e. strong links) surround those buses where highest number of cascading events take place. These

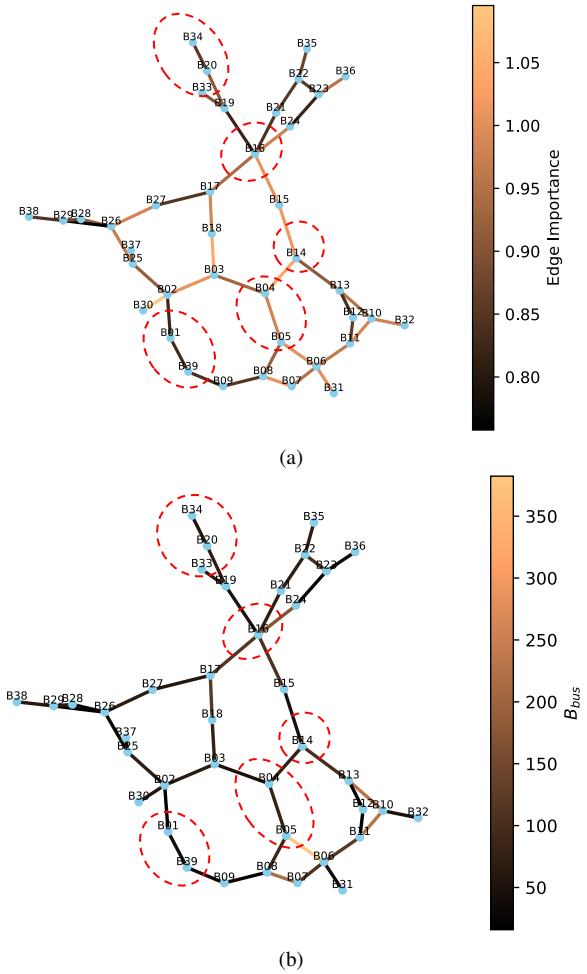

Fig. 3: Modified IEEE 10 machine 39 bus test-system (a) DFC graph (b)Y_{bus} (ignoring line conductances) based graph

buses (or at most their 1-hop and/or 2-hop neighbours) are linked together with strong edges in the DFC graph. On the contrary, the Y-bus based graph shown in Fig. 3(b), only detects two of these sub-graphs (around $B16$ and $B05$) amongst the five sub-graphs where highest number of cascading events occur. It is important to note that, in addition to the sub-graphs where most number of failures take place, the DFC graph also reveals few other strongly connected sub-graphs which might not be captured by the simulation dataset but may be vulnerable from the perspective of cascading events. This additional information obtained from the DFC graph may be useful to harden vulnerable subgraphs for mitigating cascading events. Based on time-domain simulations and [28] the most frequently occurring sequence of CF and the reason for activation of a protection device associated with it are also recorded at the end of the time-domain simulation exercise used for generating the features for the proposed learning scheme (Section III). A snapshot of most commonly occurring CF sequences are shown in Table I. As an example, the behaviour observed in the second most common pattern, i.e. the disconnection of wind farm $NSG2$ due to overvoltage followed by the disconnection of $G1$ due to out of step protection, is linked to the graphs shown in Fig. 3(a). In Fig. 3(a), $B16$ (directly connected to $NSG2$) and $B30$ (directly connected to $G1$), are strongly connected with higher edge-weight paths in the DFC graph, but this is not the case in Y-bus based graph, as shown in Fig. 3(b). This further validates the usefulness of DFC graphs for characterising vulnerability to CF.

In to validate the effectiveness of proposed DFC graphs, node-centrality indices are calculated and visualised in Fig. 4(a)-(d). From Fig. 4(a) it can be observed that for both types of graphs, $B16$ has highest degree centrality as fault on lines connected to $B16$ (specifically Line 16-19) always leads to cascading events across the network. This is in line with the definition as *nodes with high degree centrality act as failure-spreading nodes*. A key difference here is that for the DFC graph, a large amount of centrality can be shifted into a small number of nodes in the system, e.g., the first 10 most important nodes based on the degree centrality take more than 97% of the system's total centrality. This is however not the case with degree centrality of the Y-bus based graph. The betweeness centrality of graph in Fig. 4(b) shows that node $B16$ is the most important node. Nodes having high betweenness centrality are the nodes that are on the shortest paths between a large number of pair of nodes and hence are crucial to the communication in a graph [34]. This is in line with the observation from time-domain simulations that initial fault on lines connected to node $B16$ would lead to CF in almost one-third ($\approx 31.67\%$) of the cases, out of which tripping of Line 16 - 19 leads to CF in 100% of cases. There also seem to be few other *bridge* nodes in both types of graphs, such as $B04$ and $B26$, where the betweeness centrality tends to be higher. An exception is $B39$ which has a high betweenness centrality for the DFC graph which can be correlated to high number of failure cases involving $G1$ and under-voltage tripping of wind generator, $NSG2$ due to fault on Line 1-39. This information is not evident from th Y-bus based node-centrality indices. The closeness centrality of nodes $(B14, B16, B17, B18)$ and $(B02, B03, B04)$ are highest followed by nodes $(B25, B26, B27)$ and $(B01, B39)$. These nodes constitute the load-rich regions and thus vulnerable to loss of demand as a result of CF. Lastly, eigen-vector centrality depicts node-importance in terms of the importance of its neighbours. The eigen-vector centrality of the DFC graph shows a distribution similar to degree centrality, but a sparser one. Similar to closeness centrality, eigen-vector centrality of DFC graph shows that the subgraphs formed by buses $(B02, B03, B04)$, $(B14, B16, B17)$, $(B25, B26, B27)$ and $(B37, B38, B39, B01)$ exhibit high eigenvector centrality indices. The eigen-vector centrality of nodes for the DFC graph and admittance based graph respectively are further visualised in Fig. 5(a)-(b). From Fig. 5(a) it is observed that the eigen-vector centrality of the DFC graph exhibits distinct clusters, typical of spectral clustering observed due to the dynamic phenomena than eigen-vector centrality of Y-bus based graph (Fig. 5(b)) which is dispersed "flatly"

TABLE I: Most frequently occurring sequence of cascading events

Event sequence	#pattern appeared
[(“NSG2”,* “OverVoltage”)]	2219
[(“NSG2”, “OverVoltage”), (“G1”,** “Out of step”)]	336
[(“NSG2”, “OverVoltage”), (“NSG1”, “OverVoltage”), (“G1”, “Out of step”)]	279
[(“NSG2”, “OverVoltage”), (“G1”, “Under-Speed”), (“NSG3”, “UnderVoltage”)]	243

* NSG1, NSG2, NSG3 represent wind generators, ** G1, G4, G5 represent synchronous generators.

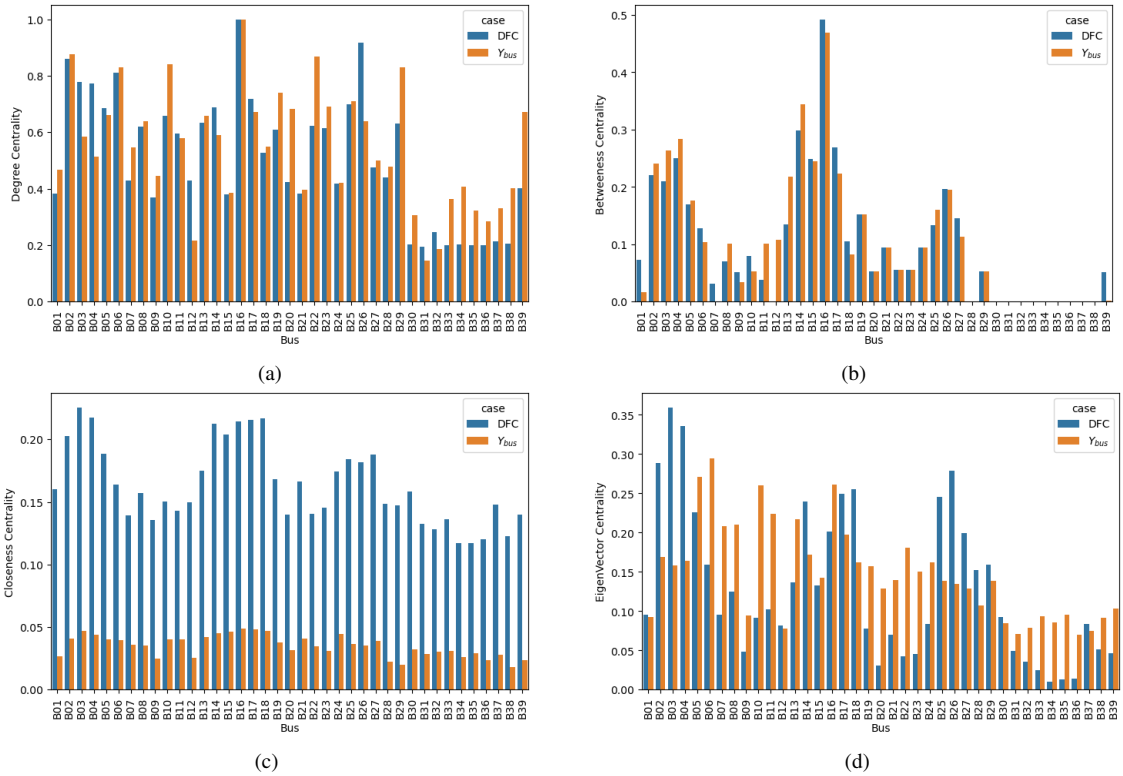

Fig. 4: Complex Network Theory based centrality indices for Y_{bus} and DFC graph (a) Degree centrality (b) Betweenness centrality (c) Closeness centrality (d) Eigen-vector centrality

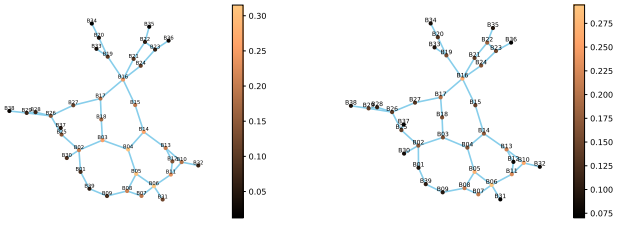

Fig. 5: Network showing eigen-vector centrality for (a) DFC graph (b) Y_{bus} graph.

across nodes. Thus, the "close” clustering of buses with high eigen-vector centrality in Fig. 5(a) can be used to discover latent clusters for the power system, with respect to their vulnerability to CF. To summarise, the DFC graph shows more detailed cascading information and more importantly identifies few key subgraphs (comprising around 10% of edges) which are only captured with the DFC graph. In order to compare the ranking of important (vulnerable) nodes - at which centrality measures are high, a more systematic approach based on rank Spearman correlation between DFC graph and Y-bus based graph is conducted as shown in Fig. 6(a)-(d). For each pair, the Spearman correlation coefficient, r and associated p-value [35], p is also shown on the plots. A high value of r signifies high rank correlation between the different centrality measures and p-value close to zero signifies high probability of refuting the null-hypothesis that the centrality measures are uncorrelated. It is evident from Fig. 6(a)-(d) that the ranks of betweeness, closeness and current-flow closeness centrality measures are highly correlated (and with a high probability), which corroborate the findings from Fig. 4(a)-(d). On the other hand, the ranks of degree and eigen-vector centrality measures are less slightly correlated. Furthermore, high standard deviation in rank correlation (shaded blue region on either side of the regression line) moving towards higher value of centrality measures in Fig. 6(a) and 6(d) also depict the dissimilarity in DFC and Y-bus based centrality measures,

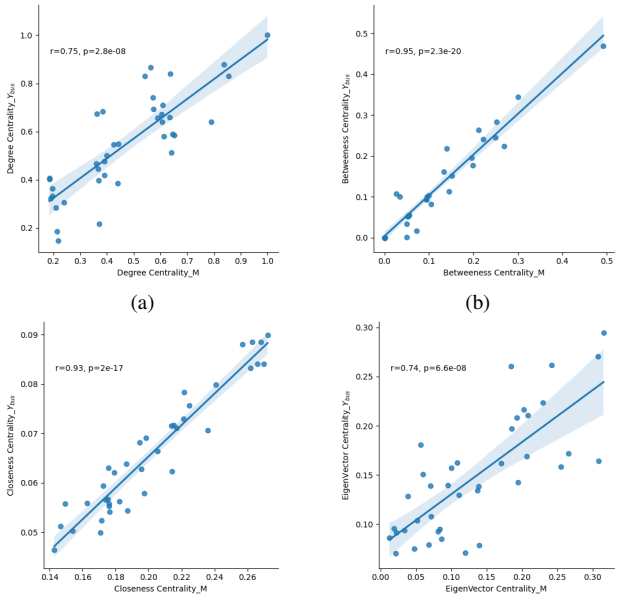

Fig. 6: Rank correlation between Complex Network Theory based centrality indices for Y_{bus} and DFC graph

thereby questioning the credibility of vulnerability analysis solely based on Y-bus.

V. Conclusion

This work proposes a spatio-temporal graph-theoretic framework for learning an augmented power system graph to assess the spatial vulnerability of power systems to cascading events. Different from those based on quasi steady-state models, the proposed graph considers the impact of collective transient dynamics of the entire system on the sequence of cascading failures. In addition to the temporal evolution of failures, the proposed framework also takes into account the topological (electrical) power system connectivity for learning - an edge-importance matrix as well the probability of occurrence of cascading events in an end-to-end manner. The learnt edge- importance matrix is further projected as power system DFC, akin to the topological connectivity. The proposed method when tested for different operational scenarios of load and RE generation on a modified IEEE 10 machine 39 bus test system, with detailed dynamic modelling including wind generation and the action of protection devices, predicts the occurrence of CF before their onset with a mean accuracy of about 97.10% and low variance. Using the learnt DFC graph it is further observed that vulnerable power system spatial locations are not only local but multi-hops away to the line where the initial triggering fault occurred. Complex network theory based indices calculated for both the DFC graph and bus-admittance based graph show good agreement (in identifying vulnerable regions) for closeness centrality. On the other hand differences between the two graphs become implicit when comparing betweenness, degree and eigenvector centrality. This demonstrates that the proposed approach can locate vulnerable spatial locations in terms of CF while taking into account the detailed dynamic phenomena. Such a graph when learnt using the proposed model utilising more types of spatio-temporal power system features such as voltage phase angles could offer valuable insights that can support better monitoring and informed decisions for system operators, in terms of mitigating cascading events. In the operational time-scale, inferences drawn using the proposed method, about spatial vulnerability to dynamic cascading failures can be used for creating better $N-k$ contingency lists than random events. Due to its fewer trainable parameters than time-series based learning methods, the usage of current framework for near real-time situational awareness also seems promising.

References

[1] J. Bialek *et al.*, "Benchmarking and validation of cascading failure analysis tools," *IEEE Trans. on Power Syst.*, vol. 31, no. 6, pp. 4887–4900, 2016.

[2] P. Henneaux, P.-E. Labeau, J.-C. Maun, and L. Haarla, "A two-level probabilistic risk assessment of cascading outages," *IEEE Trans. on Power Syst.*, vol. 31, no. 3, pp. 2393–2403, 2015.

[3] M. Vaiman, K. Bell, Y. Chen, B. Chowdhury, I. Dobson, P. Hines, M. Papic, S. Miller, and P. Zhang, "Risk assessment of cascading outages: Methodologies and challenges," *IEEE Trans on Power Syst.*, vol. 27, no. 2, p. 631, 2012.

[4] P. Rezaei, P. D. Hines, and M. J. Eppstein, "Estimating cascading failure risk with random chemistry," *IEEE Trans. on Power Syst.*, vol. 30, no. 5, pp. 2726–2735, 2014.

[5] P. D. Hines, I. Dobson, and P. Rezaei, "Cascading power outages propagate locally in an influence graph that is not the actual grid topology," *IEEE Trans. on Power Syst.*, vol. 32, no. 2, pp. 958–967, 2016.

[6] A. J. Flueck, I. Dobson, Z. Huang, N. E. Wu, R. Yao, and G. Zweigle, "Dynamics and protection in cascading outages," in *2020 IEEE PESGM*. IEEE, 2020, pp. 1–5.

[7] J. Song, E. Cotilla-Sanchez, G. Ghanavati, and P. D. H. Hines, "Dynamic modeling of cascading failure in power systems," *IEEE Trans. on Power Syst.*, vol. 31, no. 3, pp. 2085–2095, 2016.

[8] S. Mei, F. He, X. Zhang, S. Wu, and G. Wang, "An improved opa model and blackout risk assessment," *IEEE Trans. on Power Syst.*, vol. 24, no. 2, pp. 814–823, 2009.

[9] B. Park, X. Su, and K. Sun, "An enhanced opa model: Incorporating dynamically induced cascading failures," *IEEE Trans. on Power Syst.*, vol. 37, no. 6, pp. 4962–4965, 2022.

[10] P. Henneaux, J. Song, and E. Cotilla-Sanchez, "Dynamic probabilistic risk assessment of cascading outages," in *2015 IEEE Power & Energy Society General Meeting*. IEEE, 2015, pp. 1–5.

[11] K. Zhou, I. Dobson, Z. Wang, A. Roitershtein, and A. P. Ghosh, "A markovian influence graph formed from utility line outage data to mitigate large cascades," *IEEE Trans. on Power Syst.*, vol. 35, no. 4, pp. 3224–3235, 2020.

[12] R. S. Biswas, A. Pal, T. Werho, and V. Vittal, "A graph theoretic approach to power system vulnerability identification," *IEEE Trans. on Power Syst.*, vol. 36, no. 2, pp. 923–935, 2020.

[13] J. Qi, K. Sun, and S. Mei, "An interaction model for simulation and mitigation of cascading failures," *IEEE Trans. on Power Syst.*, vol. 30, no. 2, pp. 804–819, 2015.

[14] E. Cotilla-Sanchez, P. D. Hines, C. Barrows, and S. Blumsack, "Comparing the topological and electrical structure of the north american electric power infrastructure," *IEEE Systems Journal*, vol. 6, no. 4, pp. 616–626, 2012.

[15] Z. Wang, A. Scaglione, and R. J. Thomas, "Electrical centrality measures for electric power grid vulnerability analysis," in *49th IEEE Conference on Decision and Control (CDC)*, 2010, pp. 5792–5797.

[16] E. Bompard, R. Napoli, and F. Xue, "Extended topological approach for the assessment of structural vulnerability in transmission networks," *IET GTD*, vol. 4, no. 6, pp. 716–724, 2010.

[17] J. Yan, H. He, and Y. Sun, "Integrated security analysis on cascading failure in complex networks," *IEEE Trans. on Information Forensics & Security*, vol. 9, no. 3, pp. 451–463, 2014.

[18] A. Torres and G. Anders, "Spectral graph theory and network dependability," in *2009 Fourth International Conference on Dependability of Computer Systems*. IEEE, 2009, pp. 356–363.
[19] A. Nasiruzzaman and H. Pota, "Modified centrality measures of power grid to identify critical components: method, impact, and rank similarity," in *2012 IEEE PESGM*. IEEE, 2012, pp. 1–8.
[20] J. Fang, C. Su, Z. Chen, H. Sun, and P. Lund, "Power system structural vulnerability assessment based on an improved maximum flow approach," *IEEE Trans. on Smart Grid*, vol. 9, no. 2, pp. 777–785, 2016.
[21] J. W. Simpson-Porco, F. Dörfler, and F. Bullo, "Voltage collapse in complex power grids," *Nature communications*, vol. 7, no. 1, p. 10790, 2016.
[22] A. E. Motter, S. A. Myers, M. Anghel, and T. Nishikawa, "Spontaneous synchrony in power-grid networks," *Nature Physics*, vol. 9, no. 3, pp. 191–197, 2013.
[23] T. Ahmad and P. N. Papadopoulos, "Prediction of cascading failures and simultaneous learning of functional connectivity in power system," in *2022 IEEE PES Innovative Smart Grid Technologies Conference Europe*. IEEE, 2022, pp. 1–5.
[24] S. Yan, Y. Xiong, and D. Lin, "Spatial temporal graph convolutional networks for skeleton-based action recognition," in *Proc. of the AAAI conference on AI*, vol. 32, no. 1, 2018.
[25] T. N. Kipf and M. Welling, "Semi-supervised classification with graph convolutional networks," *arXiv preprint arXiv:1609.02907*, 2016.
[26] Y. Chen, L. Wu, and M. Zaki, "Iterative deep graph learning for graph neural networks: Better and robust node embeddings," *Advances in neural information processing systems*, vol. 33, pp. 19 314–19 326, 2020.
[27] S. M. Blair, M. H. Syed, A. J. Roscoe, G. M. Burt, and J.-P. Braun, "Measurement and analysis of pmu reporting latency for smart grid protection and control applications," *IEEE Access*, vol. 7, pp. 48 689–48 698, 2019.
[28] G. A. Nakas, A. Dirik, P. N. Papadopoulos *et al.*, "Online identification of cascading events in power systems with renewable generation using measurement data and machine learning," *IEEE Access*, 2023.
[29] A.-A. B. Bugaje, J. L. Cremer, and G. Strbac, "Generating quality datasets for real-time security assessment: Balancing historically relevant and rare feasible operating conditions," *International Journal of Electrical Power & Energy Systems*, vol. 154, p. 109427, 2023.
[30] A. Paszke *et al.*, "Pytorch: An imperative style, high-performance deep learning library," in *Advances in Neural Information Processing Systems 32*. Curran Associates, Inc., 2019, pp. 8024–8035.
[31] B. Park, X. Su, and K. Sun, "An enhanced opa model: Incorporating dynamically induced cascading failures," *IEEE Transactions on Power Systems*, vol. 37, no. 6, pp. 4962–4965, 2022.
[32] S. Gharebaghi, N. R. Chaudhuri, T. He, and T. La Porta, "An approach for fast cascading failure simulation in dynamic models of power systems," *Applied Energy*, vol. 332, p. 120534, 2023.
[33] A. Cini, I. Marisca, F. M. Bianchi, and C. Alippi, "Scalable spatiotemporal graph neural networks," in *Proceedings of the AAAI conference on artificial intelligence*, vol. 37, no. 6, 2023, pp. 7218–7226.
[34] C. Caro-Ruiz and E. Mojica-Nava, "Centrality measures for voltage instability analysis in power networks," in *2015 IEEE 2nd Colombian Conference on Automatic Control*, 2015, pp. 1–6.
[35] M. G. Kendall, "The advanced theory of statistics." 1943.